Thermochemical Surface Engineering of Stainless Steels With Interstitials; Symbiosis of Science, Technology and Innovation

Somers, Marcel A. J.; Christiansen, Thomas L.

Published in:
Proceedings.26th IFHTSE Congress 2019. International Congress on Metal Science and Heat Treatment, dedicated to the 180th Anniversary of Dmitry Chernov

Publication date:
2019

Document Version
Peer reviewed version

THERMOCHEMICAL SURFACE ENGINEERING OF STAINLESS STEELS WITH INTERSTITIALS; SYMBIOSIS OF SCIENCE, TECHNOLOGY AND INNOVATION

Marcel A.J. Somers, Thomas L. Christiansen– Technical University of Denmark, Department of Mechanical Engineering, Building 425, DK 2800 Kongens Lyngby, Denmark
somers@mek.dtu.dk, tch@mek.dtu.dk

Thermochemical surface engineering of stainless steels with carbon and nitrogen atoms was originally considered bad practice, because these elements would readily bind to chromium and thereby compromise the stainless character of the steel. The 80-ies and 90-ies of the previous century saw the introduction of low and high temperature routes for thermochemical surface engineering of stainless steels, without the formation of chromium carbides/nitrides. These routes are currently known as low temperature surface hardening (LTSH) and high temperature solution nitriding (HTSN), respectively. The present contribution addresses the scientific understanding, the technological feasibility and the innovative materials solutions related to dissolving interstitials in stainless steels. This is illustrated with examples from our own research group and combines experimental and numerical approaches.

KEYWORDS: STAINLESS STEEL–THERMOCHEMICAL–SURFACE ENGINEERING – EXPANDED AUSTENITE– NITRIDING – CARBURIZING

INTRODUCTION

Surface hardening of stainless steel by gaseous processes has long been considered bad practice and was already in the late 1940s commercially known as Malcomizing. Good practice thermochemical surface engineering of austenitic stainless steels emerged in the mid-80ies as a surface engineering technology to mitigate wear and galling, while retaining, or even improving, the (pitting and crevice) corrosion performance of this class of metals. Carburizing in carbon-enriched liquid alkali baths (today known as Kolsterizing®) [1] and plasma-assisted nitriding [2] were among the first processes. As compared to conventional carburizing/nitriding processing occurs at relatively low temperature to prevent the nucleation of chromium-based carbides/nitrides during treatment (cf. Fig. 1) and the resulting loss of corrosion resistance. Scientifically, the microstructural features responsible for surface hardening of austenitic stainless steels were poorly understood. For many years, and sometimes even today, the surface-adjacent region affected by carbon/nitrogen was referred to as S-phase [3], suggesting that a new phase develops at the surface. Later, it became apparent that, essentially, the case developing during low temperature surface hardening (LTSH) consists of a supersaturated solid solution of interstitials in an f.c.c. parent lattice. The supersaturation is enabled by chromium's affinity for C/N and the slow diffusion of substitutionally dissolved elements at the process temperature, which effectively retards carbide/nitride precipitation. Throughout the 90-ies, all published scientific studies on LTSH dealt with plasma-based treatment of stainless steels. The plasma treatment was considered essential for the removal of the passive layer from stainless steels. Unfortunately, the plasma-assisted investigations only allowed the synthesis of graded systems with steep gradients in composition and associated residual stresses. This obscured an actual interpretation of the nature of the case. The 00-s saw the emergence of gas-based processes for carburizing [4], nitriding and nitrocarburizing [5], where the passive film was removed or transformed during a pre-treatment or, preferably, as an integrated part of the treatment. This enabled precise control of the temperature and composition of the C/N-providing medium, thus opening up for targeted surface engineering.

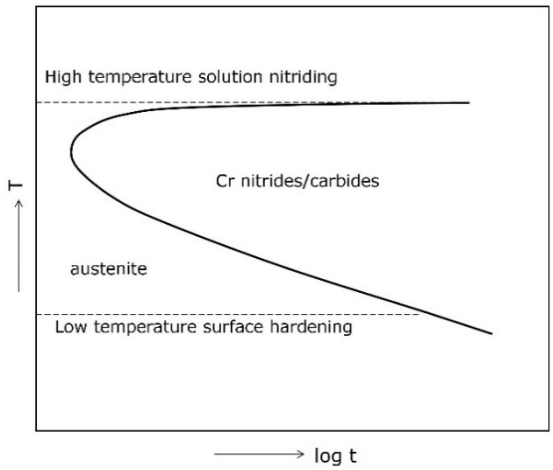

Fig.1 - Schematic TTT diagram showing high temperature solution nitriding (HTSN) is performed at a temperature where no nitrides/carbides are stable; low temperature surface hardening (LTSH) is performed at a temperature where it takes a long time before nitrides/carbides nucleate.

Another development is the surface engineering of austenitic, ferritic, martensitic and duplex stainless steels, which was initiated by Berns [6,7] in the 90-ies and is currently known as high temperature solid solution nitriding (HTSN). Here, the treatment temperature is in a range where Cr-based nitrides and carbides are not stable (cf. Fig. 1) and an appreciable amount of nitrogen can be dissolved in austenite at high temperature, typically above 1050 °C. The HTSN treatment can be applied to austenitic, martensitic, ferritic and duplex stainless steels [7] and should be followed by fast cooling to prevent the development of chromium nitrides (cf. Fig. 1) that would compromise the corrosion performance.
The present contribution highlights some of the scientific, technological and innovative aspects of LTSH and HTSN, as obtained in our research group.

LOW TEMPERATURE SURFACE HARDENING OF AUSTENITIC STAINLESS STEEL

The identity of the supersaturated solid solution of interstitials (nitrogen and carbon) in austenitic stainless steels has been under discussion for 35 years, since the first publications by Kolster [1] and Zhang and Bell [2]. It appears now widely accepted that this supersaturated solid solution is not a separate phase, but that the lattice of metal atoms remains f.c.c., while nitrogen and carbon atoms are dissolved in the octahedrally coordinated interstices. As compared to the major alloying elements Fe and Ni, Cr has a stronger affinity to C and particularly N. Therefore, in the supersaturated solid solution short range ordering (SRO) occurs between Cr and N/C [8,9]. For very high interstitial contents, as for N, long-range ordering (LRO) of the interstitials can occur in addition to the aforementioned SRO [10]. Recent research indicates that the LRO is commensurate with LRO in γ'-Fe_4N, albeit that combined SRO and LRO leads to over-stoichiometry as compared to the ratio M:N=4:1 (where M represents all metallic elements in the f.c.c. lattice of the alloy, i.e. Fe,Cr,Ni,Mo), implying that the N content exceeds 20 at.%; this LRO has been dubbed γ'_N [12]. Typical examples of micrographs of expanded austenite cases stabilized by carbon, nitrogen or nitrogen and carbon are given in Fig. 2.

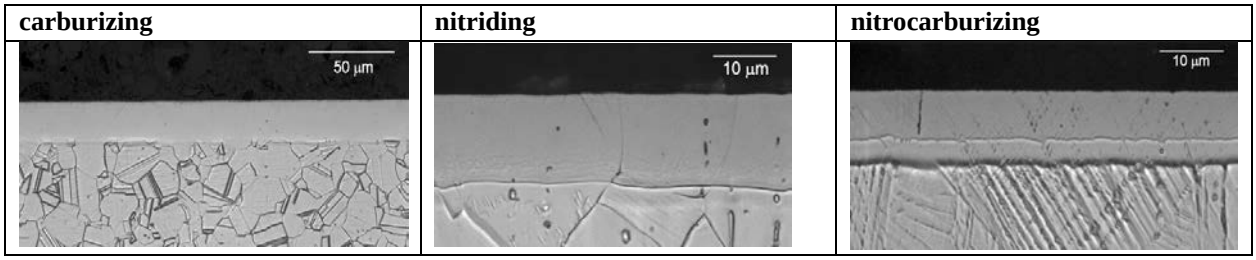

Fig. 2 - Micrographs of cross sections of carburized, nitrided and nitrocarburized AISI 316 (304 for the nitrocarburized specimen). Conditions were as follows: carburizing in C_2H_2- H_2-N_2 at 783 K for 3 h [12]; nitriding at 718 K for 22 h in 60% NH_3-40% H_2 [13]; nitrocarburizing at 693 K for 19h in 14% C_3H_8-54 % NH_3-22% H_2- 10% Ar [12].

The micrographs show an almost featureless case, because the electrochemical properties of expanded austenite are improved as compared to the initial stainless steel. Grain boundaries from the steel are observed to continue in the case, consistent with the interpretation that no new phase develops. Orientation image maps (OIMs) as determined with electron back-scatter diffraction (EBSD) for a nitride sample indicate that the expanded austenite case is characterized by a rotation of the original lattice, which is evidence that plastic deformation has occurred under the dissolution of a high content of interstitial elements (Fig. 3) [14].

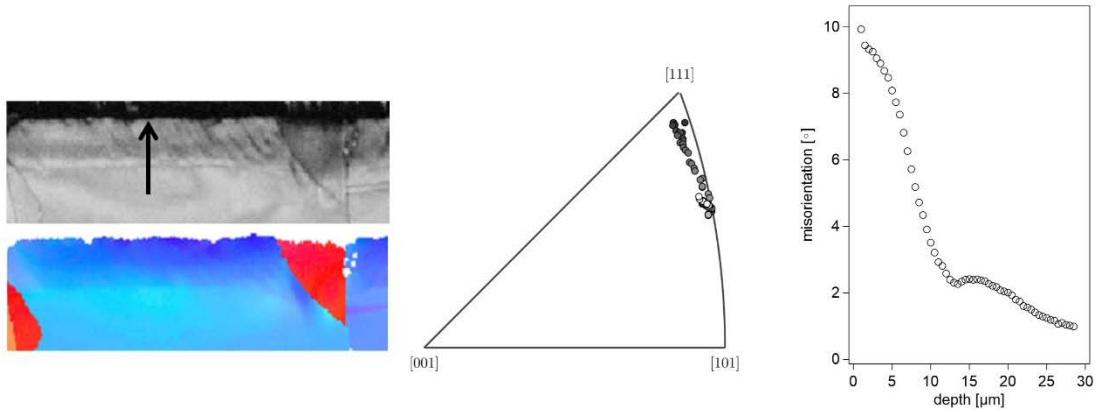

Fig. 3 - Image quality maps (top left) and orientation image maps (bottom left) as obtained from EBSD investigation of AISI 316 nitrided at 713 K for 8 h in NH_3. The dots on the orientation triangle (middle) show the lattice rotation from substrate (white dots) to surface (black dots) along the arrow indicated in the top row; corresponding quantitative misorientation (right) [14].

Such plastic deformation as a response to a mere change in composition, can be understood as follows. The dissolution of interstitials in an f.c.c. lattice leads to a lattice expansion. For low interstitial contents this lattice expansion can be accommodated by compressive elastic strains (residual stress) in the case. Along with the dissolution of interstitials, solid solution strengthening occurs leading to an increase of the yield strength. With increasing interstitial content the residual stresses can become so high that they locally exceed the increase of the yield strength and, accordingly, plastic deformation occurs. Such plastic deformation has been observed in polycrystalline materials by the appearance of slip lines at the surface [15,16] and is most clearly illustrated on the surface of initially polished single crystals of stainless steel 316 (Fig. 4) [17]. For a crystal with <001> perpendicular to the surface quadratic patterns emerge, because four {111} slip planes intersect with the {001} surface; for a <111> oriented single crystal (or grain) triangular patterns emerge, as three {111} slip planes intersect with the surface.

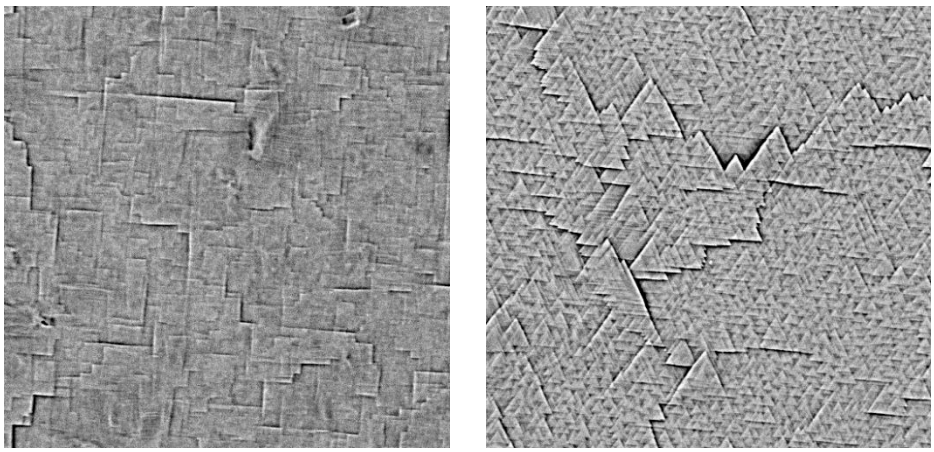

Fig. 4 - Surface of single crystals of AISI 316L after nitriding at 693 K in a gas mixture of 80% NH_3 and 20 % H_2; left <001>, right <111>. Quadratic (left) and triangular (right) patterns are the result of dislocation slip along {111} intersection with the surface. Note that no lattice rotation occurs for <001> and <111> [17].

The residual stresses in expanded austenite have been determined with X-ray diffraction analysis. As a consequence of the occurrence of gradients in both stress and composition as well as strong elastic and plastic anisotropy, it is not a straightforward task to accurately determine residual stresses. An overview of the various procedures to deal with these

conditions was provided in [14] and references therein. Residual stresses in nitrogen stabilized expanded austenite (γ_N) on AISI 316 are maximally (in compression) -5 GPa, while for carburized AISI 316 about -2.7 GPa [18] was determined. These huge elastic stresses are far beyond the yield stress of stainless steel and indicate that considerable strengthening has been achieved by dissolving interstitials.

Numerical simulation of the development of composition and stress profiles during nitriding (or carburzing) requires consideration of concentration-dependent diffusion of nitrogen in the f.c.c. lattice and the incorporation of elasto-plastic accommodation, including strengthening, of the volume expansion. A numerical model, incorporating thermal, chemical and mechanical coupling was developed [19, 20], which allows the prediction of nitrogen concentration as well as elasto-plastic and thermal strain distributions from thermodynamic, crystallographic, diffusion and thermal expansion (and magnetic properties) data for expanded austenite. By means of example the composition, residual stress and elastic, plastic and thermal strains calculated for 3 different nitriding times in pure NH_3 are shown in Fig. 5 [14].

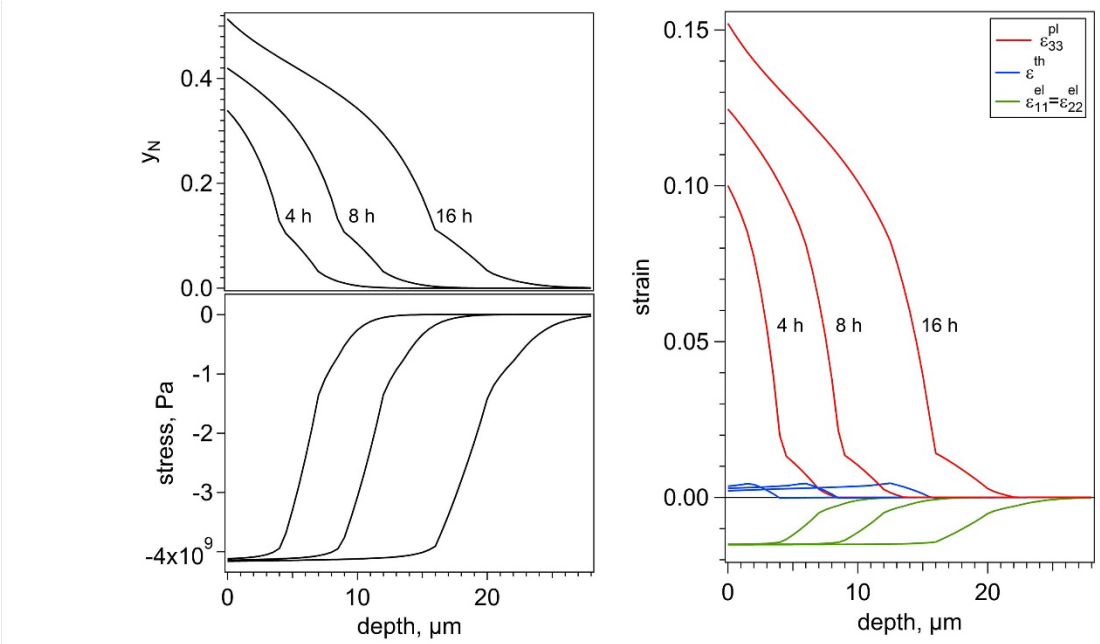

Fig. 5 – Calculated evolutions of nitrogen content (expressed as the number of N atoms per 100 metal atoms, y_N), residual stress as well as elastic, plastic and thermal strains in AISI 316 for 3 different nitriding times at 713 K in pure NH_3 [14].

Comparison of the plastic strains in Fig. 5 (red lines) with the misorientation profile by plastic deformation in Fig. 3, shows an encouraging qualitative agreement between the experimental and predicted profiles. It was demonstrated recently that there is a quantitative discrepancy between the predicted and experimental evolutions of the composition (and associated strain) profiles, which can be attributed to the role of the surface reaction (ammonia dissociation) in controlling the nitrogen transfer from the gas to the solid state [20]. In this sense, the developed multi-physics numerical model can be used to further explore the role of the surface reaction and optimize the gaseous treatment such that shorter treatment times can be realized under practical conditions.

The model can also be applied to plasma nitriding [20] and gaseous carburizing [21]. An example of the latter is shown in Fig. 6. Here, X-ray diffraction was used to determined both the carbon content in solid solution and the associated residual stress. The carbon concentration profile was fitted with a diffusion model, as accurate diffusion coefficients for carbon in expanded austenite are unavailable. From the carbon concentration profile, which essentially is the strain-free volume expansion of the austenite lattice, the residual stresses were calculated assuming elasto-plastic accommodation of the expansion. To this end, elastic (Young's modulus) and plastic (yield strength and work hardening coefficient) properties were assessed from nano-indentation. An excellent quantitative correspondence was obtained between thus calculated and measured residual stresses [21].

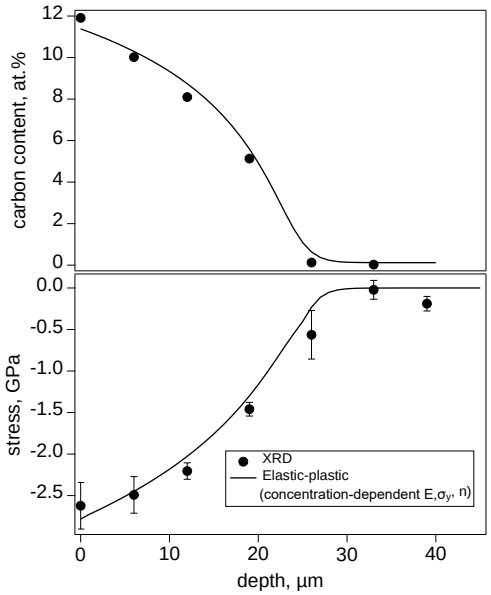

Fig. 6 – Carbon content and residual stress determined with X-ray diffraction on expanded austenite in AISI 316L carburized for 30 h at 743 K in a CO-H_2 gas mixture [21].

HIGH TEMPERATURE SOLUTION NITRIDING OF STAINLESS STEEL

In contrast to LTSH in a gaseous environment, where it was necessary to activate the surface by stripping the passive layer prior to treatment, dissolving nitrogen during HTSN is straightforward as Cr-oxide evaporates as CrO_3 in this temperature regime [22]. Moreover, N_2 gas dissociates at the stainless steel surface, hence nitrogen can directly be dissolved. The equilibrium nitrogen content that can be dissolved is determined by the alloy composition, the applied temperature and the (total or partial) N_2 pressure in the gas [7]. An example of the relation between temperature and gas pressure is shown in the isopleth for AISI 316 in Fig. 7a [23]. HTSN at 1400 K in 0.25 bar N_2 yields an equilibrium solubility of 0.30 wt% N. The case depth that is achieved can be several hundreds of microns deep. This allows the development of a thick austenite case on stainless steels, or for components made from sheet, an enhanced nitrogen content throughout the thickness. As a matter of fact HTSN is an attractive alternative means to synthesize high-nitrogen steels. The motivation for applying an HTSN treatment could be the enhanced corrosion resistance that is achieved, because N has an important influence on the PREN or MARC number of stainless steels [24]. Fig. 7b illustrates that in particular the pitting potential is importantly improved after HTSN of AISI 316 for different N_2 pressures, giving the N contents provided in the legend to Fig. 7b.

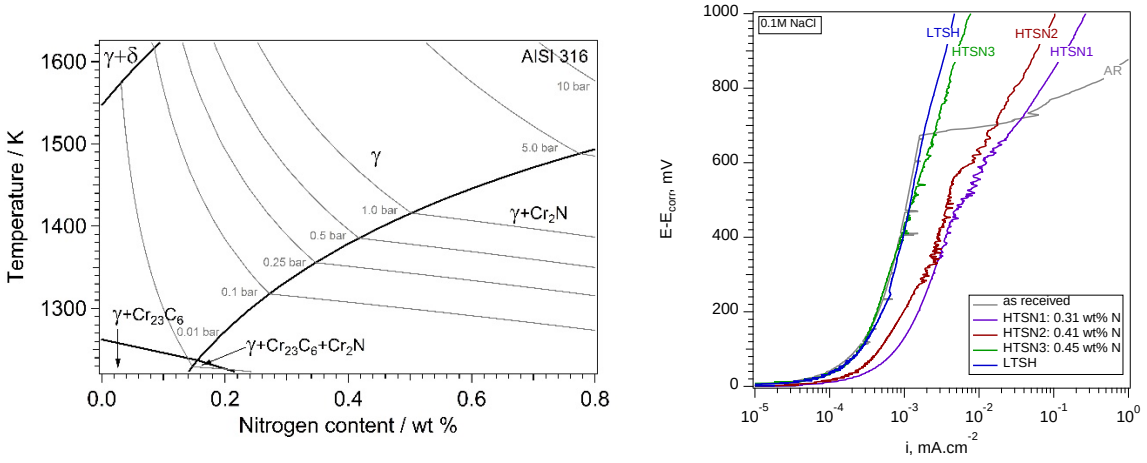

Fig. 7 – a. (left) Isopleth (black lines) of AISI 316 in the high temperature range for increasing nitrogen content; isobars (grey lines) of N_2 pressure are superimposed [23]; b. (right) polarization diagrams with respect to the corrosion potential (E_{corr}) for AISI 316 in as-received, HTSN (for 3 N_2 pressures) and LTSH condition [25].

Another motivation for HTSN is an increase of the hardness and yield strength. An example of the change of the mechanical properties is given in Fig. 8 [23]. The combination of alloy composition, nitrogen content and degree of deformation can establish a wide range of hardness values (Fig. 8a). Clearly, the yield strength and the work hardening coefficient of AISI 316 and AISI 304L are drastically changed, while ductility is maintained (Fig. 8b).

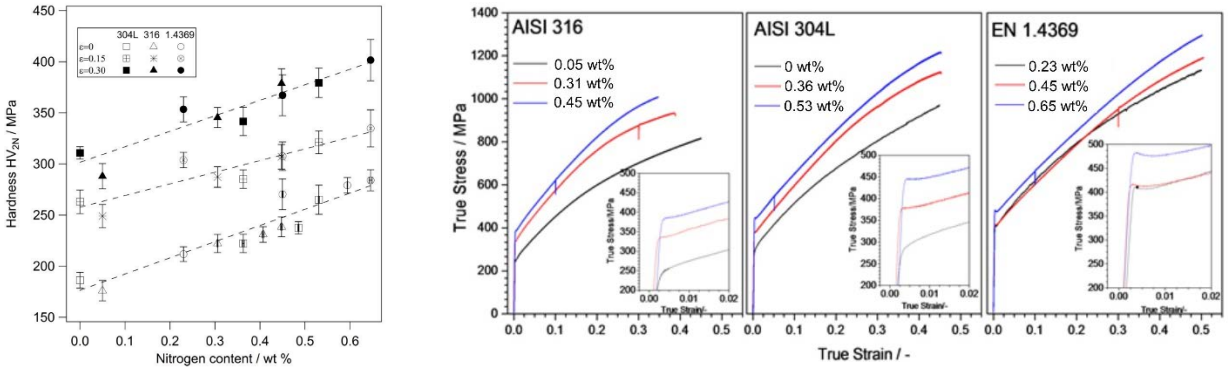

Fig. 8 – a. (left) hardness at 2N load measured in AISI 316/304L and EN 1.4369 for different combinations of nitrogen content obtained by HTSN and tensile straining (see legend); b. (right) tensile testing curves for as received (black lines) and HTSN treated (red and blue lines) AISI 316/304L and EN 1.4369 [23].

An important effect of nitrogen on austenite is a modification of the stacking fault energy (SFE). Although the exact relation between N content and SFE is not accurately known, the considerable stabilization of austenite against strain-induced martensite formation upon deformation widens the application potential of these alloys. This is the main reason for the difference in the tensile curves for AISI 316/ 304L on the one hand side and EN 1.4369 on the other (Fig. 8b). The former two alloys develop strain-induced martensite upon tensile straining, while the latter already contains 0.23 wt% N and is stable in the as-received state. Thus, HTSN of EN 1.4369 does not change the tensile behavior as pronouncedly as for AISI 304L/316. The enhanced stability of austenite and the prevention of strain-induced martensite on plastic deformation opens up for innovative forming applications. Strain-induced martensite negatively influences the corrosion performance of stainless steel and is particularly harmful during LTSH, where it promotes CrN precipitation . Stabilizing austenite by a prior HTSN treatment, allows deformation by plastic forming (bending or embossing) or shot peening to promote high strength (cf. Fig 8b) or compressive residual stresses to improve fatigue performance, while retaining the corrosion performance. An example of extreme deformation by surface roller burnishing is given in Fig. 9 [27].

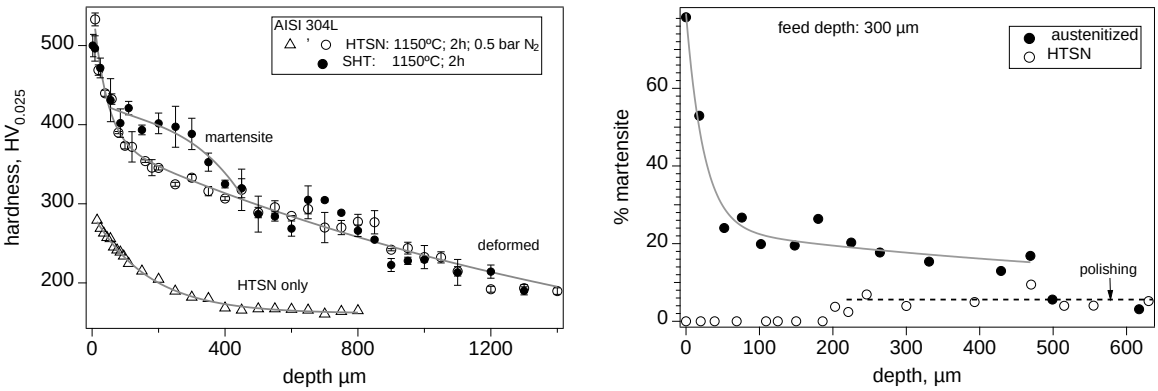

Fig. 9 – Hardness (load 25g), measured in cross section, and martensite content (determined with XRD and successive layer removal) as a function of depth for solution heat treated (SHT), i.e. austenitized, and HTSN treated AISI 304L after surface roller burnishing. The martensite in the roller burnished HTSN treated sample is a result of mechanical polishing necessary to enable XRD as a function of depth [27].

In the surface near region, the material is nano-crystalline, while at larger depth twinning and/or martensite (both α' and ε) formation occurs depending on the nitrogen content and corresponding SFE [27].

HTSN can also be a very effective treatment prior to deformation and subsequent LTSH by nitriding, carburizing or nitrocarburizing [27]. Here, the HTSN case has several advantages:

- it provides enhanced load-bearing capacity for the expanded austenite zone (cf. Fig. 8 or, after deformation, Fig. 9);
- it provides a gradual change in the electrochemical properties (cf. Fig. 7b) and consequently, excellent, corrosion performance;
- it avoids formation of strain-induced martensite and associated CrN development on LTSH, which was demonstrated to yield excellent uniformity of LTSH independent of the degree of deformation [23].

Finally, the rapid evolution of additive manufacturing, in particular 3D printing of stainless steels, requires targeted heat and surface treatment to mitigate the unconventional and hierarchical microstructure (Fig. 10), which has poor corrosion resistance. Here, the combination of HTSN and LTSH has been demonstrated to provide excellent improvement of wear performance and restauration of the corrosion performance [29].

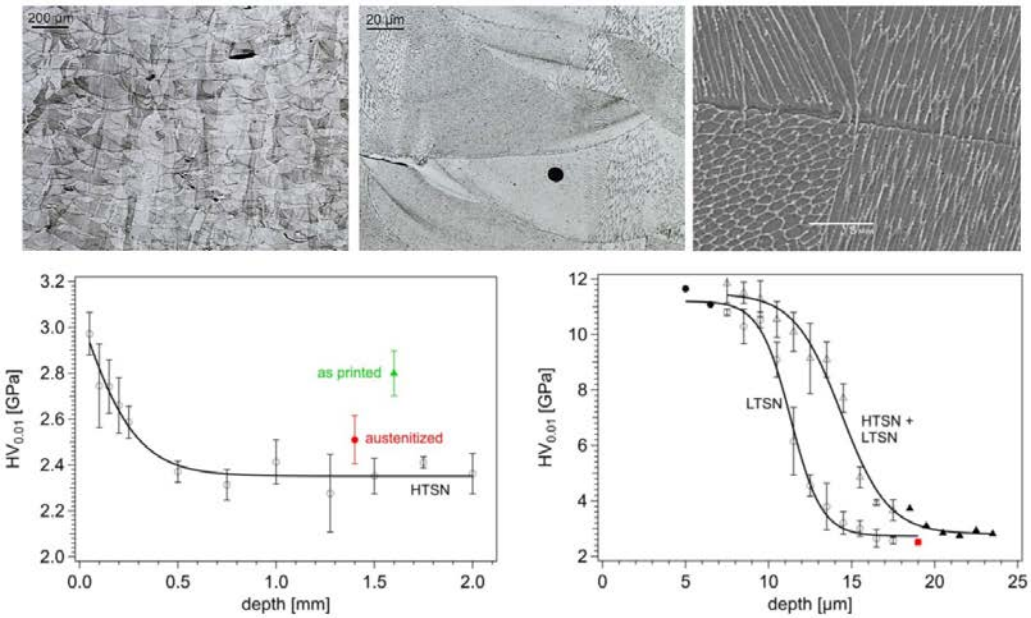

Fig. 10 – Hierarchical microstructure (top row) of selective laser melted AISI 316L, showing, from left to right, elongated grains, weld lines and cell structure. The cell structure is dissolved upon austenitizing, leading to a hardness decrease, which for HTSN is counteracted in the surface region. Low temperature surface nitriding (LTSN), provides a hardened case, with a surface hardness (load 10g) of 11 GPa [29].

As is clear from the examples given in this article, the LTSH and HTSN treatments are currently applied to the most widely applied austenitic stainless steels. Certainly, process variants for other types of stainless steels are also available. What all stainless steels have in common is that they were never intended to be surface treated by LTSH of HTSN, but they derive their application from a combination of corrosion performance, deformability, strength, and for the case of martensitic qualities, wear resistance. In the last 30 years the metallurgical understanding of the interplay between LTSH/ HTSN and the stainless steel microstructure has reached a level that allows the design of stainless alloy compositions that are targeted to exploit the many beneficial aspects of these treatments [30]. These alloys could be considered pendants to special carburizing and nitriding steels. In particular, the enormous scientific attention that high-entropy alloys currently receive, may contribute to inspire in which direction these stainless nitriding and carburizing steels should be developed.

CONCLUSION

Thermochemical surface engineering of stainless steels with interstitials has evolved into high temperature and low temperature variants. The various processing technologies allow dissolution of controlled quantities of carbon and nitrogen into stainless steels. The scientific understanding has reached maturity and shows that in particular the nitrided

case formed at low temperatures is extremely complex. Thus formed expanded austenite contains (steep) gradients in composition, residual stress, texture, and degrees of deformation and magnetization. The complexity is reflected in a thermochemical/mechanical multi-physics numerical model that enables simulation of composition and stress profiles from the treatment parameters temperature, time and gas composition, and takes all the elasto-plastic straining into account. Interstitials in stainless steels have a large influence on the mechanical properties (hardness and yield strength) and improve the localized corrosion performance. Combinations of high and low temperature treatments, including (intermediate) plastic deformation enable innovative materials solutions, where strength, load bearing capacity, wear performance and corrosion performance are improved. The metallurgical understanding of the processing is ready for the post-treatment of innovative AM (3D print) components and the development of stainless carburizing and nitriding steels.

ACKNOWLEDGEMENT

Over the years several PhDs and Postdocs and numerous MSc students have contributed importantly to various aspects of the work presented. We are grateful to Thomas S. Hummelshøj, Jette Oddershede, Bastian K. Brink, Federico Bottoli, Frederico A.P. Fernandes, Freja N. Jespersen, Ömer C. Kücükyildiz, Yawei Peng, Emilie H. Valente and Bo Wang for their valuable research contributions. Also, the collaborations with our (former) colleagues Kenny Ståhl, Grethe Winther, Hossein Alimadadi, Jesper H. Hattel, Kristian V. Dahl, Morten S. Jellesen, Steffen S. Munch and Flemming B. Grumsen are highly appreciated.

REFERENCES

1. Kolster BH. Verschleiß- und korrosionsfeste Schichten auf austenitischen Stählen. VDI-Berichte 1983; 503: 107-113.
2. Zhang ZL, Bell T. Structure and corrosion resistance of plasma-nitrided stainless steel. Surf Eng 1985; 1: 131-136.
3. Dong H. S-phase surface engineering of Fe-Cr, Co-Cr and Ni-Cr alloys. Int Mater Rev 2010; 55: 65-98.
4. Collins S, Williams P. Adv Mater Proc 2006; 164:32-33.
5. Christiansen T, Somers MAJ. Low temperature gaseous nitriding and carburizing of stainless steel. Surf Eng 2005; 21: 445-455.
6. Berns H. Patents DE 403 3706 A1 1990 and DE 433 3917 A1, 1994
7. Berns H. Stainless steels suited for solution nitriding. Mat-wiss u Werkstofftech 2002; 33: 5-11.
8. Oddershede J, Christiansen TL, Ståhl K, Somers MAJ. Extended X-ray absorption fine structure investigation of nitrogen stabilized expanded austenite. Scripta Mater. 2010; 62: 290-293.
9. Oddershede J, Christiansen TL, Ståhl K, Somers MAJ. Extended X-Ray Absorption Fine Structure Investigation of Carbon Stabilized Expanded Austenite and Carbides in Stainless Steel AISI 316. Steel Res Int. 2011; 82: 1248-1254.
10. Brink B, Christiansen TL, Hansen MF, Frandsen C, Somers MAJ. Composition-dependent variation of magnetic properties and interstitial ordering in homogeneous expanded austenite. Acta Mater. 2016; 106: 32-38.
11. Che HL, Tong S, Wang KS, Lei MK, Somers MAJ. Co-existence of γ'_N phase and γ_N phases on nitrided austenitic Fe-Cr-Ni alloys- I. Experiment. Acta Mater. submitted.
12. Christiansen T, Hummelshøj TS, Somers MAJ. Gaseous Carburising of self-passivating Fe-Cr-Ni alloys in acetylene-hydrogen mixtures. Surf Eng 2011; 27: 602-608.
13. Christiansen T, Somers MAJ. Controlled dissolution of colossal quantities of nitrogen in stainless steel. Metall Mater Trans A 2006; 37: 675-682.
14. Somers MAJ, Kücükyildiz OC, Ormstrup C, Alimadadi H, Christiansen TL, Winther G. Residual stress in expanded austenite on stainless steel; origin, measurement and prediction. Mater Perf Char 2018; 7: 693-716.
15. Fewell MP, Mitchell DRG, Priest JM, Short KT, Collins GA. The nature of expanded austenite. Surf Coatings Techn 2000;131: 300-306.
16. Templier C, Stinville JC, Villechaise P, Renault PO, Abrasonis G, Rivière JP, Martinavičius A, Drouet M. On lattice plane rotation and crystallographic structure of the expanded austenite in plasma nitrided AISI 316L steel. Scripta Mater. 2010; 63: 496-499.
17. Kücükyildiz OC, Grumsen FB, Christiansen TL, Winther G, Somers MAJ. Low temperature gaseous nitriding of single crystals of stainless steel; the role of elastic and plastic anisotropy-I. Experimental. in preparation
18. Christiansen TL, Somers MAJ. Stress and composition of carbon stabilized expanded austenite on stainless steel. Metall Mater Trans A 2009; 40:1791-1798.

19. Jespersen FN, Hattel JH, Somers MAJ. Modelling the evolution of composition- and stress-depth profiles in austenitic stainless steels during low-temperature nitriding. Mod Sim Mater Sci Eng 2016; 25: 025003 (31 pages).
20. Kücükyildiz OC, Sonne MR, Thorborg J, Somers MAJ, Hattel JH. Thermo-chemical mechanical simulation of low temperature gas and plasma nitriding of austenitic stainless steel; inverse modelling of surface reaction rates. Mod Sim Mater Sci Eng. submitted.
21. Peng Y, Liu Z, Jiang Y, Wang B, Gong JM, Somers MAJ. Experimental and numerical analysis of residual stress in carbon-stabilized expanded austenite. Scripta Mater. 2018; 157:106-109.
22. Caplan D, Cohen M. The volatilization of chromium oxide, J Electrochem Soc 1961; 108: 438-442.
23. Bottoli F, Winther G, Christiansen TL, Dahl KV, Somers MAJ. Low-temperature nitriding of deformed austenitic stainless steels with various nitrogen contents obtained by prior high-temperature nitriding. Metall Mater Trans A 2016; 47: 4146-4159.
24. Speidel MO. Nitrogen containing austenitic stainless steels. Mat-wiss u Werkstofftech 2006; 37: 875-880.
25. Bottoli F, Jellesen MS, Christiansen TL, Winther G, Somers MAJ. High temperature solution-nitriding and low-temperature nitriding of AISI 316: Effect on pitting potential and crevice corrosion performance. Appl Surf Sci 2018; 431: 24-31.
26. Bottoli F, Winther G, Christiansen TL, Somers MAJ. Influence of plastic deformation on low-temperature surface hardening of austenitic stainless steel by gaseous nitriding. Metall Mater Trans A 2016; 46: 2579-2590.
27. Wang B, Hong CS, Christiansen TL, Somers MAJ. in preparation.
28. Christiansen TL, Hummelshøj TS, Somers MAJ. Patents WO 2012 146254-A1 and WO 2013 159781-A1.
29. Valente EH, Christiansen TL, Somers MAJ. High-temperature solution nitriding and low-temperature surface nitriding of 3D printed austenitic stainless steel. Proc. European Conference on Heat Treatment (ECHT) Nitriding and Nitrocarburizing 2018: 71-80.
30. Christiansen TL, Dahl KV, Somers MAJ. New Stainless Steel Alloys for Low Temperature Surface Hardening, Berg- und Hüttenmännische Monatshefte 2015; 160: 406-412.